Available online at www.sciencedirect.com
SCIENCE DIRECT®
Biomaterials 25 (2004) 4087–4103
Biomaterials
www.elsevier.com/locate/biomaterials

Effects of topography and composition of titanium surface oxides on osteoblast responses

Xiaolong Zhu[a,*], Jun Chen[a], Lutz Scheideler[a], Rudolf Reichl[b], Juergen Geis-Gerstorfer[a]

[a] Department of Prosthodontics and Medical Materials, Section of Medical Materials and Technology, University of Tuebingen, Osianderstr. 2–8, Tuebingen D-72076, Germany

[b] NMI Natural and Medical Science Institute at the University of Tuebingen, Markwiesenstr. 55, Reutlingen D-72770, Germany

Received 23 June 2003; accepted 11 November 2003

Abstract

To investigate the roles of composition and characteristics of titanium surface oxides in cellular behaviour of osteoblasts, the surface oxides of titanium were modified in composition and topography by anodic oxidation in two kinds of electrolytes, (a) 0.2 M H_3PO_4, and (b) 0.03 M calcium glycerophosphate (Ca-GP) and 0.15 M calcium acetate (CA), respectively. Phosphorus (P: ca.10 at%) or both calcium (Ca: 1–6 at%) and phosphorus (P: 3–6 at%) were incorporated into the anodized surfaces in the form of phosphate and calcium phosphate. Surface roughness was slightly decreased or enhanced (R_a in the range of 0.1–0.5 μm) on the anodized surfaces. The geometry of the micro-pores in the anodized surfaces varied with diameters up to 0.5 μm in 0.2 M H_3PO_4 and to 2 μm in 0.03 M Ca-GP and 0.15 M CA, depending on voltages and electrolyte. Contact angles of all the anodic oxides were in the range of 60–90°. Cell culture experiments demonstrated absence of cytotoxicity and an increase of osteoblast adhesion and proliferation by the anodic oxides. Cells on the surfaces with micro-pores showed an irregular and polygonal growth and more lamellipodia, while osteoblasts on the titanium surface used as a control or on anodic oxides formed at low voltages showed many thick stress fibres and intense focal contacts. Alkaline phosphatase (ALP) activity of the cells did not show any correlation with surface characteristics of anodic oxides.

Keywords: Topography; Chemical composition; Titanium oxides; Osteoblasts; Cell culture; Anodic oxidation

1. Introduction

The biocompatibility of titanium as an implant material is attributed to surface oxides spontaneously formed in air and/or physiological fluids [1]. Cellular behaviours, e.g. adhesion, morphologic change, functional alteration, proliferation and differentiation are greatly affected by surface properties, including composition, roughness, hydrophilicity, texture, and morphology of the oxide on titanium [2,3]. The natural oxide is thin (about 3–8 nm in thickness) and amorphous, stoichiometrically defective. It is known that the protective and stable oxides on titanium surfaces are able to provide favourable osseointegration [4,5]. The stability of the oxide depends strongly on the composition, structure and thickness of the film [6]. As a consequence, great efforts have been devoted to thickening and stabilizing surface oxides on titanium to achieve desired biological responses.

The nature of the surface oxides can be manipulated by thermal oxidation and/or anodic oxidation. In vitro and in vivo studies show that alterations in the surface oxide of titanium implants strongly influence the tissue response [7]. The oxide film formed by thermal oxidation is typically thin due to its slow formation process by O_2 diffusion through the titanium oxide film. In contrast, anodic oxidation is efficient to control the thickness, composition and topography of the oxide film on titanium [8–10] and can be applied for implant surface modification.

Among surface properties, surface roughness and composition have been considered the most important parameters for altering cell activity [11]. The biological response to titanium depends on the surface chemical

*Corresponding author. Tel.: +49-7071-29-80967; fax: +49-7071-29-5775.
E-mail address: xiaolong.zhu@med.uni-tuebingen.de (X. Zhu).

0142-9612/$ - see front matter © 2003 Elsevier Ltd. All rights reserved.
doi:10.1016/j.biomaterials.2003.11.011

composition, and the ability of titanium oxides to absorb molecules and incorporate elements [12]. Surface topography plays a fundamental role in regulating cell behaviour, e.g. the shape, orientation and adhesion of cells [13–15]. As a surface begins to contact with biological tissues, water molecules first reach the surface. Hence, surface wettability, initially, may play a major role in adsorption of proteins onto the surface, as well as cell adhesion. Cell adhesion is generally better on hydrophilic surfaces. It is known that changes in the physicochemical properties, which influence the hydrophilicity of Ti dioxide will modulate the protein adsorption and further cell attachment [16]. By anodic oxidation, elements such as Ca and P can be imported into the surface oxide on titanium and the microtopography can be varied through regulating electrolyte and electrochemical conditions. The presence of Ca-ions has been reported to be advantageous to cell growth [17,18], and in vivo data show implant surfaces containing both Ca and P enhance bone apposition on the implant surface [19]. Although in vitro and in vivo studies have shown that the anodic oxides of titanium demonstrate positive biological responses [20,21], no detailed in vitro biological responses have been investigated to anodic oxides with different compositions and topographies. Since micro-pores of anodic oxides are comparable with biological entities in size, the biological interactions induced by such surfaces would most likely be different from those occurring on the flat surface.

As titanium with high-energy stable natural or anodic oxides is well known for its strong affinity to ambient elements such as oxygen, hydrogen, nitrogen, and carbon, absorption of ubiquitous hydrocarbon always occurs under normal conditions in air or solution containing organic contaminants. Surface contamination can be produced during the processing of titanium such as machining, surface treatment and sterilization. Surface contamination could be responsible for the loss of an implant a few of years after surgery [22]. More attentions have been paid to probably negative effects from surface contamination, and different chemical and physical cleaning techniques are applied to decontaminate titanium implants. It is reported that initial implant surface free energy and surface cleaning play a significant role in the healing and generation of host-tissue cells adjacent to the implant surface [22,23]. In vitro studies indicate that surface contamination lowers the percent of cell attachment and spreading [24].

In the present study, to evaluate effects of surface characteristics and composition of anodic oxides of titanium on osteoblast responses, various anodic oxides on titanium were prepared and biologically tested in vitro. Additionally, chemical compositions and states of the elements, morphologies, roughness and contact angles were analysed on the anodic oxides. Biological responses to the oxides which were investigated include the metabolic activity, cell adhesion, proliferation and alkaline phosphatase (ALP) activity.

2. Materials and methods

2.1. Preparation of specimens

Rectangular specimens with $20 \times 10 \times 1$ mm in size were cut from cp titanium plate (ASTM B265 GR. 2) (TITANIA Products, Essen, Germany). The pre-treatment procedure was that specimens were mechanically polished to sandpaper No. 1200, etched by mixed HF/HNO_3 solution, and cleaned by ethanol and deionized water, then air-dried. In electrolyte No. 1: 0.2 M H_3PO_4 solution [8] and electrolyte No. 2: the mixture of 0.03 M calcium glycerophosphate (Ca-GP) and 0.15 M calcium acetate (CA) [10], respectively, the dried surfaces were oxidized using a dc power supply at galvanostatic mode with current density 70 A/m^2. The temperature was maintained at 20°C by water bath during anodic oxidation. Specimens were rinsed with deionized water and dried with nitrogen gas immediately after being anodized. With different voltages of anodic oxidation, the specimens were divided into eight groups as follows:

Group 1: pretreated Ti as a control (G-1);

Group 2: pretreated Ti and anodized in 0.2 M H_3PO_4 till 200 V (G-2);

Group 3: pretreated Ti and anodized in 0.2 M H_3PO_4 till 300 V (G-3);

Group 4: pretreated Ti and anodized in 0.2 M H_3PO_4 till 350 V (G-4);

Group 5: pretreated Ti and anodized in 0.03 M Ca-GP and 0.15 M CA till 140 V (G-5);

Group 6: pretreated Ti and anodized in 0.03 M Ca-GP and 0.15 M CA till 200 V (G-6);

Group 7: pretreated Ti and anodized in 0.03 M Ca-GP and 0.15 M CA till 260 V (G-7);

Group 8: pretreated Ti and anodized in 0.03 M Ca-GP and 0.15 M CA till 300 V (G-8).

In the procedure of cleaning and sterilization, specimens were ultrasonically cleaned in 70% ethanol for 15 min, washed in deionized water, and air dried under a laminar flow hood. Culturing and harvesting of cells were performed exactly as described for the specimens of all the groups.

2.2. Surface characteristics

The surface roughness of the prepared specimens was quantified using a surface profilometer (Perthometer S6P, Perthen Instruments, Mahr, Goettingen, Germany). A 2-μm diamond stylus was used to determine the centreline average roughness along a 5.6 mm length. Five individual measurements, between which the distance was 200 μm, were made for each specimen to

obtain accurate data of surface roughness. Maximum roughness within the distance measured (R_{max}), mean value of five single measurements within the distance examined (R_Z) and the arithmetical mean of surface roughness of every measurement within the total distance (roughness average $= R_a$) were assessed.

The prepared specimens were coated with a thin layer of Au–Pd film for electric conductivity by plasma deposition, and subsequently scanning electron microscope (SEM) (Leo 1430) was used to observe the topography of the prepared specimens.

Surface composition and elemental states of prepared specimens were determined quantitatively with VG ESCALAB 200 X-ray photoelectron spectroscopy (XPS) using a Mg anode.

The contact angle can characterize the wettability of the surface of a solid by a liquid, i.e. the interaction between a solid and a liquid surface at the interface, and represent a thermodynamic relationship known as the Young equation, which relates the angle θ to the interfacial solid–vapour (SV), solid–liquid (SL) and liquid–vapour (LV) free energies (γ) as follows: $\gamma_{SV} = \gamma_{SL} + \gamma_{LV}\cos\theta$.

Prepared specimens were kept in air for more than two months so as to stabilize the contact angle. Contact angles were measured on DSA 10Mk 2 (Kruess) equipped with a video-imaging system. Sessile deionized-water drops were placed on the surface in the ambient environment, with drop volumes of 5 μl. Images were recorded during 3 min and five images every second with a video system, and the contact angle values were calculated by analysing drop shape using the drop shape analysis system (DSA 1) and selected at 10 s.

2.3. Cell culture

The SaOS-2 human osteoblast-like cell line, derived from a human osteosarcoma, was obtained from the DSMZ (German Collection of Microorganisms and Cell Cultures). Cells were cultured in modified McCoy's 5A medium (Sigma-Aldrich Chemie GmbH, Taufkirchen, Germany) containing 10% fetal calf serum (FCS; PAA Laboratories GmbH, Linz, Austria), 1% penicillin (10,000 units)/streptomycin (10 mg/ml, GIBCO, Scotland, UK) and 1% 200 mM L-glutamine (PAA Laboratories GmbH, Linz, Austria) and maintained in humidified atmosphere with 5% CO_2 at 37°C. The culture medium was renewed twice one week. When cells reached confluence, a diluted Trypsin-EDTA (0.5 g/l Trypsin and 0.2 g/l EDTA, GIBCO, Scotland, UK) was used to detach cells from the bottom of the culture flasks and 1/3 of total cells were transferred into a new tissue culture flask.

2.3.1. Cytotoxicity

Cytotoxicity tests were performed by an extract method. Extracts of all specimens were obtained from contact of samples with modified McCoy's 5A cell culture medium for 72 h at 37°C (according to ISO 10993-5). The ratio between sample surface and the volume of the extraction vehicle was 3 cm^2/ml. SaOS-2 osteoblast-like cells at a concentration of 5000 cells/well were seeded in a 96-well plate in 150 μl modified McCoy's 5A medium per well. After 24 h the medium was discarded and replaced by the extracts derived from the different samples. Each extract was tested in three concentrations: (i) undiluted (150 μl), (ii) 1:2 diluted with medium (50 + 100 μl) and (iii) 1:14 diluted (10 + 140 μl). Cell culture medium without extraction was used as the negative control. A toxic PVC-film (Rehau GmbH, Germany) was extracted in the same manner as the samples and used as positive control. After additional 24 h of culture, cytotoxicity was assayed by XTT-Test (cell proliferation Kit, Roche Diagnostics GmbH, Mannheim, Germany).

The assay is based on the cleavage of the yellow tetrazolium salt XTT (sodium 3′-[1-(phenylaminocarbonyl)-3,4-tetrazolium]-bis(4-methoxy-6-nitro) benzene sulphonic acid hydrate) (Roche Diagnostics GmbH, Mannheim, Germany) to form an orange formazan dye by metabolically active cells. Therefore, this conversion only occurs in viable cells. The formazan dye formed is soluble in aqueous solutions and is directly quantified using a scanning multiwell spectrophotometer (ELISA reader).

2.3.2. Cell attachment and spreading

Cell attachment was assessed by seeding SaOS-2 cells in a density of 2.0×10^4 cells/cm^2 for 1 and 2 h on the surfaces of specimens. After 1 or 2 h, respectively, the specimens were rinsed with phosphate-buffered saline (PBS Dulbecco's, Scotland, UK) without magnesium and calcium, fixed with 2% paraformaldehyde in PBS for 15 min at room temperature, immersed in 1% Triton X-100 in PBS for 5 min, and then blocked with 5% goat serum at room temperature. Vinculin, one kind of proteins related to focal contacts, was stained with mouse anti-human-vinculin (Sigma-Aldrich Chemie GmbH, Steinheim, Germany) as primary antibody and TRITC (tetramethylrhodamine isothiocyanate) conjugated anti-mouse-IgG (Sigma-Aldrich Chemie GmbH, Steinheim, Germany) as secondary antibody. For staining of actin filaments, fixed cells were incubated with FITC-conjugated phalloidin. After fluorescent staining, the specimens were mounted with fluorescence protection mounting medium (Polyvinyl alcohol mounting medium with DABCO; Fluka Chemie GmbH, Buchs, Switzerland) and evaluated in an epifluorescent microscope (Nikon-OPTIPHOT-2, Nikon Co., Japan).

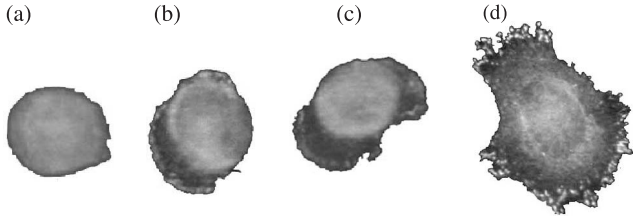

Fig. 1. All the pictures of cells in this figure were from the present experiment. All attached cells were divided into (a) not spread: cells were still spherical in appearance, protrusions or lamellipodia were not yet produced; (b) and (c) partially spread: at this stage, cells began to spread laterally at one or more sides, but the extensions of plasma membrane were not completely confluent; (d) fully spread: extension of plasma membrane to all sides, combined with distinctly larger surface area than in stages a to c and obvious flattening of the cell, was observed.

Cell attachment and spreading was assessed by microscopic examination of all samples by one trained examinator. As shown in Fig. 1, all attached cells were divided into (a) not spread: cells were still spherical in appearance, protrusions or lamellipodia were not yet produced; (b) and (c) partially spread: at this stage, cells began to spread laterally at one or more sides, but the extensions of plasma membrane were not completely confluent; (d) fully spread: extension of plasma membrane to all sides, combined with distinctly larger surface area than in stages a to c and obvious flattening of the cell, was observed [25]. The number of total attached cells and percentage of fully spread cells among attached cells were calculated from 5 different random areas (0.8×0.8 mm) of each specimen. The mean number of attached cells on the surfaces of the control (cp Ti, G-1) for 1 h cell culture was set as 100%, and the data of the other groups were compared with it. Focal contact sites and cytoskeleton were examined by a Nikon E950 digital Camera (Nikon Co., Japan) under fluorescence microscopy.

2.3.3. Cell proliferation

Each group of specimens used for cell proliferation tests was divided into three subgroups and measured after cell culturing for 1, 2 and 4 days, respectively. SaOS-2 cells were cultured on specimen surfaces with the initial cell density of 2.0×10^4 cells/cm^2 in 6-well culture plates. At every harvest time point, cells were detached from specimen surfaces by incubation with trypsin/EDTA (0.5 g/l trypsin and 0.2 g/l EDTA, GIBCO, Scotland, UK) for 5 min at 37°C, and each specimen was washed with PBS without magnesium and calcium. According to our preliminary tests, the procedure was repeated one more time to confirm no residual cells on surfaces of specimens after this releasing procedure. Released cells were counted with a hemocytometer, and on every specimen counting was repeated three times.

2.3.4. Alkaline phosphatase activity

After cell proliferation test, the cells were collected by centrifugation with 1100 rpm at room temperature for 3 min. The cell pellets were lysed in 400 μl 0.5% Triton, and alkaline phosphatase (ALP) activity was measured using p-nitrophenylphosphate (Sigma Diagnostics, Inc, St. Louis, USA) as substrate. A standard solution from p-nitrophenol (Sigma Diagnostics, Inc, St. Louis, USA) reacted with 0.1 N NaOH was diluted into a series of standard concentrations with distilled water (Ampuwa, Fresenius Kabi Deutschland GmbH, Bad Homburg, Germany) as references for measurement. Absorbance was measured using an ELISA reader with the wavelength of 405 nm. The value of ALP activity was normalized by the total cell number obtained from proliferation tests, and ALP activity was defined as nMol/min/10^4 cells.

2.3.5. Statistical analysis

All data were analysed by JMP Version 5.01 statistical analysis program (SAS Institute Inc., Cary, NC). Significant differences between all the groups and the control were determined using Dunnett's test, which guards against the high alpha size (type I) error rate across the hypothesis tests. Tukey–Kramer HSD (honestly significant difference) test was used to perform multiple comparisons between the groups anodized in the same electrolyte. The Tukey–Kramer HSD test provides a conservative calculation of statistical significance in the analysis of intergroup comparisons that minimizes the risk of type I error by increasing the quantile multiplied into the standard error values to create the least significant difference. Unless otherwise indicated, all data presented were mean $\pm$S.D. and the significance level of 0.05 (alpha) was accepted.

3. Results

3.1. Surface characterization

The morphology of the prepared groups was analysed by SEM in Fig. 2. The control surface had parallel grooves oriented along the polishing direction. The surfaces G-2 and G-5 displayed island-shaped films. The increase of the anodizing voltage resulted in the gradual formation of the anodic oxide film, i.e. from islands to the whole surface, with more and larger irregular micropores generated by sparking during anodic oxidation. The grooves produced by polishing were removed gradually as the voltage rose. The detailed studies on topography of anodized surfaces with the applied voltage are investigated in the previous work [8,10]. The pore geometry (up to ca. 0.5 μm for G-4 in diameter) in electrolyte No. 1 was distinctly smaller than that (up to 2 μm for G-8) in electrolyte No. 2.

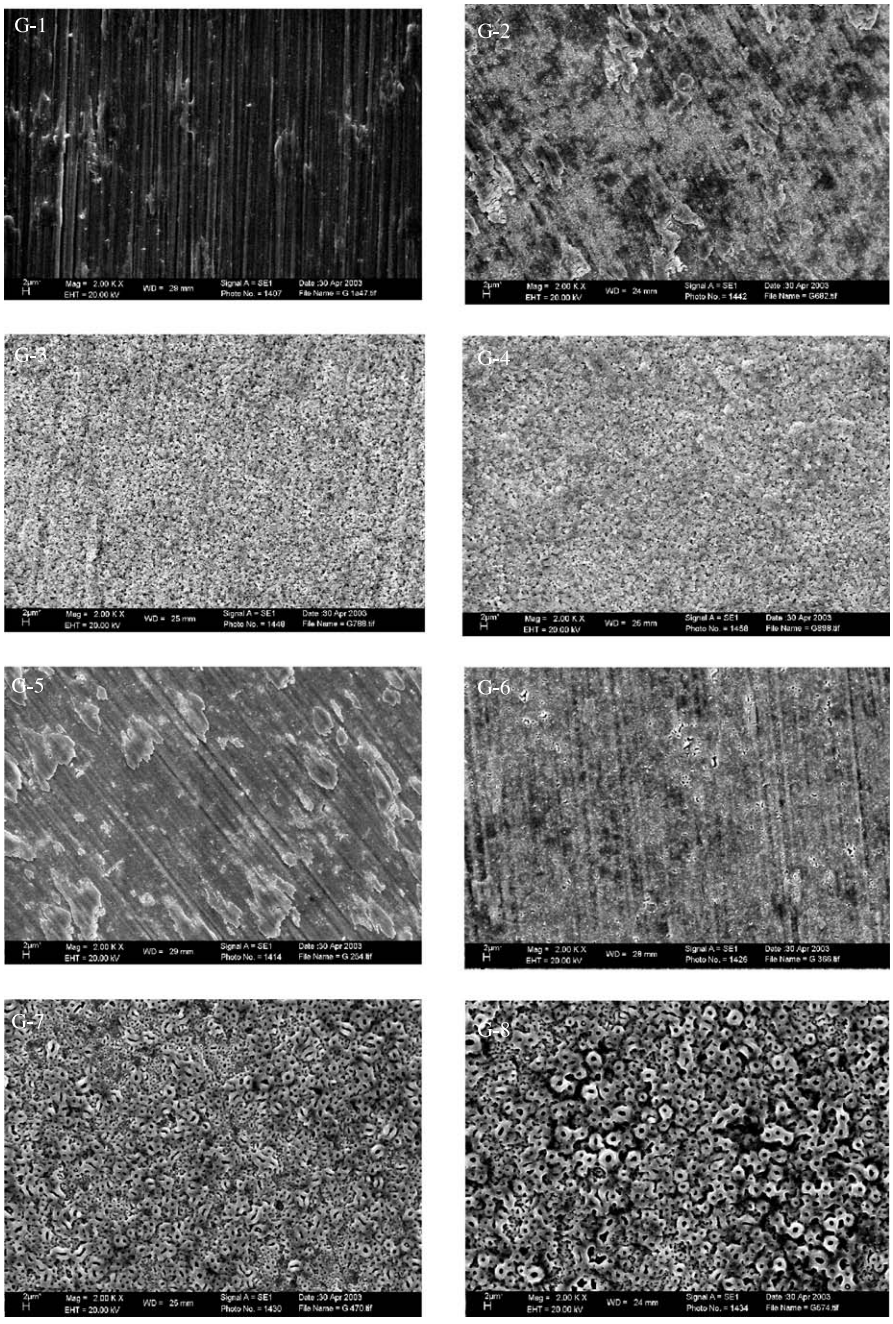

Fig. 2. Morphology of the different surfaces of titanium, anodizing conditions: 70 A/m^2, (G-1) pretreated; (G-2) at 200 V in 0.2 M H_3PO_4; (G-3) at 300 V in 0.2 M H_3PO_4; (G-4) at 350 V in 0.2 M H_3PO_4; (G-5) at 140 V in 0.03 M Ca-GP and 0.15 M CA; (G-6) at 200 V in 0.03 M Ca-GP and 0.15 M CA; (G-7) at 260 V in 0.03 M Ca-GP and 0.15 M CA; (G-8) at 300 V in 0.03 M Ca-GP and 0.15 M CA.

As shown in Fig. 3, statistical analyses indicate a influence of the anodizing voltage used on surface roughness in both electrolyte solutions tested. Significant differences are seen in electrolyte 1 between G-2 and G-3, and G-2 and G-4, respectively, and in electrolyte 2 between G-5 and G-6, G-6 and G-7, and G-7 and G-8. Therefore, the R_a value of surface roughness on anodic oxides formed in electrolyte No. 1 tended to be lower as anodizing voltage is enhanced; while in electrolyte No. 2, R_a values became higher with increasing voltage. Statistical significant difference was shown in roughness between any anodized surface and the control surface, and between the anodized surfaces formed in the same electrolyte except between G-3 and G-4. However, all the R_a values were in the range of 0.1–0.5 μm, which is similar to that of the machined surfaces [4,26]. Thus, anodic oxidation can increase the surface roughness but only to a limited extent.

Contact angle measurements indicate that the values of all contact angles of the control (untreated) and

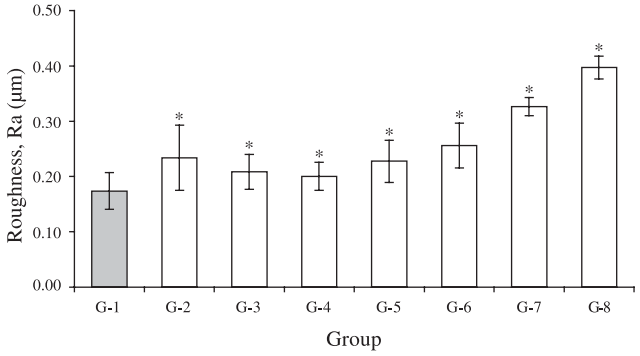

Comparisons for all pairs in the same electrolyte using Tukey-Kramer HSD (Abs(Dif)-LSD)

	G-2	G-3	G-4		G-5	G-6	G-7	G-8
G-2	-0.02411	0.00428^{+}	0.01105^{+}	G-5	-0.02078	0.00749^{+}	0.07818^{+}	0.14853^{+}
G-3	0.00428^{+}	-0.02411	-0.01734	G-6	0.00749^{+}	-0.02078	0.04991^{+}	0.12025^{+}
G-4	0.01105^{+}	-0.01734	-0.02411	G-7	0.07818^{+}	0.04991^{+}	-0.02078	0.04956^{+}
				G-8	0.14853^{+}	0.12025^{+}	0.04956^{+}	-0.02078

$^{+}$Positive values show pairs of means that are significantly different (Alpha = 0.05).

Fig. 3. Roughness, R_a, of the anodized surfaces of titanium, G-1 as a control, $^{*}p<0.05$.

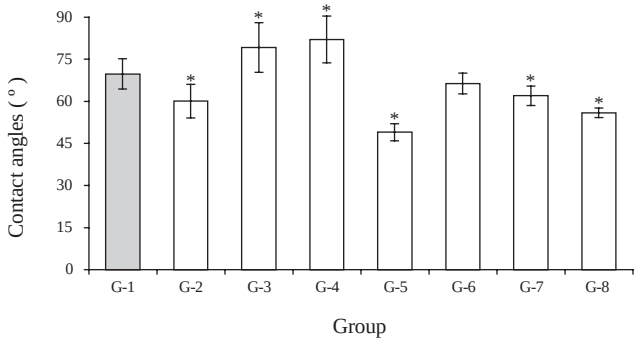

Comparisons for all pairs in the same electrolyte using Tukey-Kramer HSD (Abs(Dif)-LSD)

	G-2	G-3	G-4		G-5	G -6	G-7	G -8
G-2	-8.674	10.496^{+}	13.316^{+}	G-5	-3.707	13.663^{+}	9.323^{+}	3.243^{+}
G-3	10.496^{+}	-8.674	-5.854	G-6	13.663^{+}	-3.707	0.633^{+}	6.713^{+}
G-4	13.316^{+}	-5.854	-8.674	G-7	9.323^{+}	0.633^{+}	-3.707	2.373^{+}
				G-8	3.243^{+}	6.713^{+}	2.373^{+}	-3.707

$^{+}$ Positive values show pairs of means that are significantly different (Alpha = 0.05).

Fig. 4. Wettability of the anodized surfaces of titanium, G-1 as a control, $^{*}p<0.05$.

anodized surfaces were in the range of 60° to 90°, namely, all the surfaces were hydrophilic surfaces (Fig. 4). At higher anodizing voltages, the corresponding contact angles were higher for the anodic oxides formed in electrolyte No.1 but became lower for those formed in electrolyte No.2. The relationship of contact angles and anodising voltages exhibited a trend exactly opposite to that of surface roughness and voltages, except for G-5.

XPS analyses of the prepared groups indicate that the P content of the anodic oxides (about 10 at%) was determined by phosphate concentration in electrolyte No. 1, irrespective of anodizing voltage; while in the electrolyte No. 2, Ca content (1–6 at%) of the anodic oxides significantly increased with an increase in anodising voltage and P content (3–6 at%) was almost not affected by voltage except for at 140 V (Table 1). Ca/P ratios in anodic oxides had the trend to increase with increasing anodising voltage or thickness of oxides in

Table 1
Chemical composition of anodic oxides of titanium by XPS (at%)

Group	Ti	O	C	P	Ca	N	Si	Other[a]	Ca/P
2	10	56	18	10		1	<0.1	5	
3	7	53	23	10		2	1	4	
4	7	47	31	11		2	<0.1	<2	
5	15	55	24	3	<1	2	<0.1	1	<0.33
6	14	54	23	5	2	<1	<0.1	2	0.40
7	13	55	20	6	4	<0.1	<0.1	<2	0.67
8	12	54	20	6	6	<0.1	<0.1	<2	1.00

[a] Not clearly identified.

both electrolytes. The contaminants of carbon (20–30 at%) (C), silicon (Si) nitrogen (N) and partially oxygen (O) originate from air, the polishing and sterilization process and/or electrolytes. The chemical composition of G-1 (control), as provided by the manufacturer, consists of 0.007% N, 0.014% C, 0.002% H, 0.06% Fe, 0.150% O, residuals <0.3% in total and Ti of balance.

The Ti 2p, O 1s, C 1s, P 2p and Ca 2p XPS spectra of titanium anodic oxides formed in either electrolyte are shown in Fig. 5. The spectrometer was calibrated by using Au $4f_{7/2}$ (84.0 eV) signal. Using the C 1s main peak a charge shift of +0.9 eV has been determined. The Ti 2p peaks of anodic oxides of G-4 and G-8 were well fitted to those of Ti 2p in TiO_2 and Ti was identified to be in the form of TiO_2. In the O 1s spectra, three peaks for either G-4 or G-8 were fitted at binding energies 530.1 ± 0.2, 531.3 and 532.8 ± 0.1 eV, respectively, after correction of charge shift. The peak located at 531.3 eV corresponded to O 1 s in PO_4^{3-} [27], A second peak at 1.3 eV lower binding energy (ca. 530.1 eV) was assigned to O 1 s of TiO_2 since its binding energy was shown in the range from 529.9 to 530.9 eV [28]. The third peak at ca. 532.8 ± 0.1 was attributed to the contributions from the following probable groups, i.e. ether groups C–O or O–C–O [27,29], HPO_4^{3-} [27], basic hydroxyl [30] and chemisorbed water [31], respectively. The third peak of O 1 s became higher in G-4 compared to that in G-8, and it is ascribed to more ether groups or hydroxyl groups from electrolyte No. 2 than those from electrolyte No.1. From the C 1 s spectra, four peaks were fitted and analysed according to the literature. The predominant peak (C_0) at 284.6 eV corresponded to organic carbon (C–H, C–C), and the other three peaks with the binding energy ca.$C_0+1.5$, $C_0+3.1$, and $C_0+4.1$ eV were assigned to C–O, C=O, O–C=O, respectively [27,32]. The peak corresponding to C–O of G-8 was remarkably higher than that of G-4 and the higher peak of C–O in the surface oxide formed in electrolyte No.2 may be related to the C–O bonds of the glycerophosphate of the electrolyte. The P 2p peaks in G-4 and G-8 were well fitted at 133.3 and 133.4 eV, and assigned to phosphorus in PO_4^{3-} (at 133.4 eV) not HPO_4^{3-} (at 134.4 eV) [27]. The Ca $2p_{3/2}$ peaks in G-8 with binding

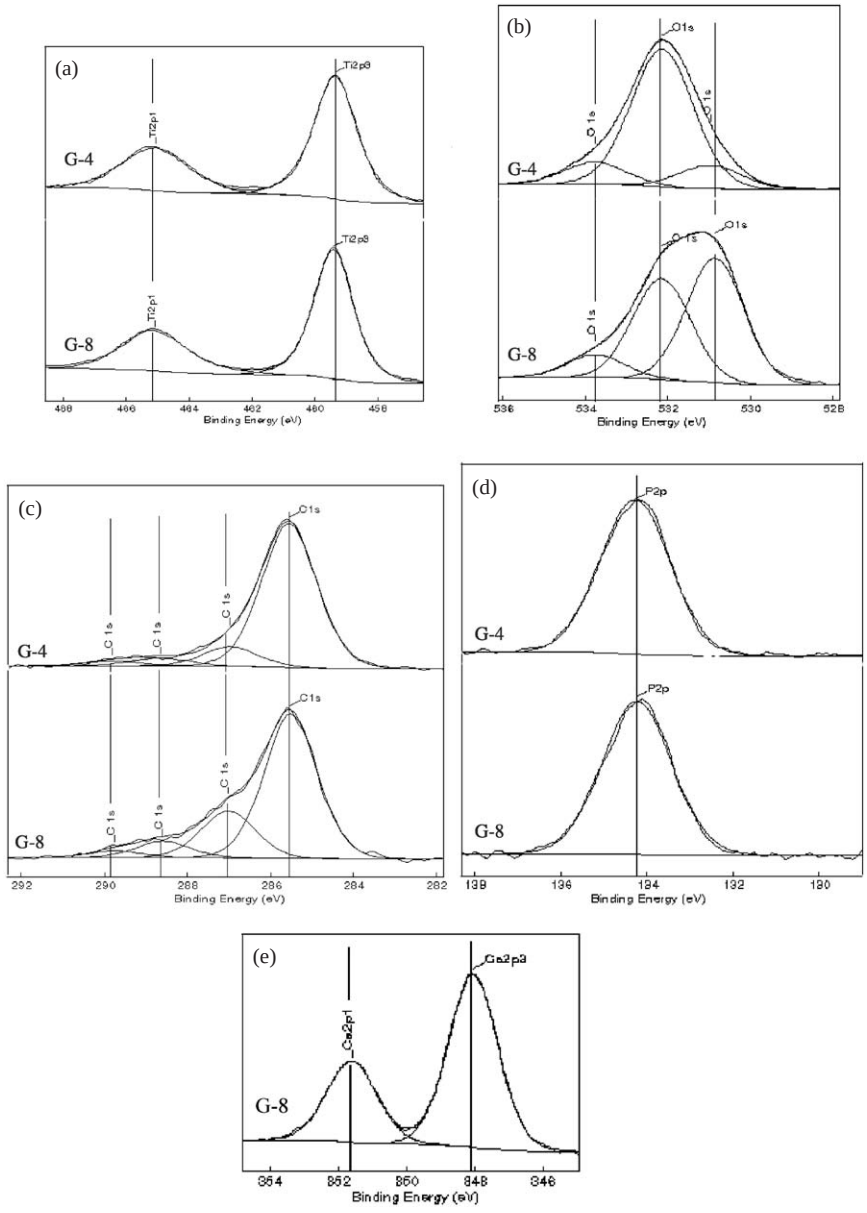

Fig. 5. High-resoultion XPS spectra of anodized surfaces of titanium (a) Ti 2p; (b) O 1s; (c) C 1s; (d) P 2p; (e) Ca 2p.

energy $2p_{3/2}$ at 347.1 eV and $2p_{1/2}$ at 350.9 eV corresponded to calcium in calcium phosphate [33] and no calcium hydroxide or calcium linked to carbonate groups was demonstrated since the corresponding Ca $2p_{3/2}$ binding energy of either of them should be much lower (ca. 345.7 eV) [27]. Besides, no information of calcium was collected in the surface oxides of G-4 due to no calcium source.

3.2. Cytotoxicity

Fig. 6 shows the cytotoxicity of extracts from all sample groups, expressed as decrease in metabolic activity of cells. No statistical significant difference in metabolic activity was shown between negative control and any tested group, while the concentration-dependent decrease in metabolic activity of the positive control (PVC) demonstrates the sensitivity of the assay. Consequently, anodized titanium surfaces with different contents of P or Ca and P do not reduce the viability and metabolism of osteoblasts.

3.3. Cell attachment and spreading

At 1 and 2 h, statistical analysis shows that the number of cells attached on nearly all the anodized oxides was apparently higher than on the surface of the control (Fig. 7), that is, initial cell attachment was enhanced by anodic oxidation. The surfaces formed at

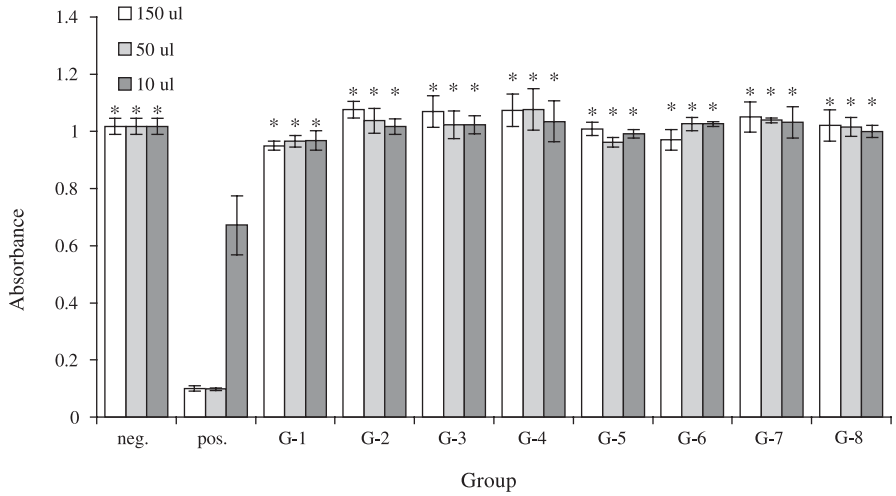

Fig. 6. Cytotoxicity of extracts of cp Ti and anodized titanium determined with SaOS-2 osteoblasts at different extract dilutions by XTT-assay. Pure cell culture medium was used as a negative control and an extract from toxic PVC as a positive control, There was significant statistical difference between the positive control and all the groups and no statistical difference between the negative control and all the groups, $*p<0.05$.

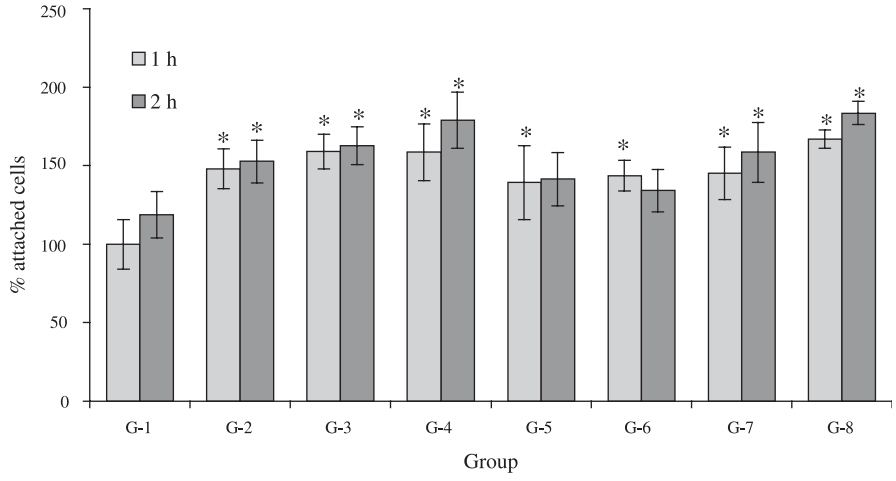

Comparisons for all pairs in the same electrolyte using Tukey-Kramer HSD (Abs(Dif)-LSD) (2 h)

	G-2	G-3	G-4		G-5	G-6	G-7	G-8
G-2	-24.743	-14.499	1.599[+]	G-5	-26.956	-19.638	-9.884	14.994[+]
G-3	-14.499	-24.743	-8.645	G-6	-19.638	-26.956	-2.566	22.312[+]
G-4	1.599[+]	-8.645	-24.743	G-7	-9.884	-2.566	-26.956	-2.078
				G-8	14.994[+]	22.312[+]	-2.078	-26.956

[+] Positive values show pairs of means that are significantly different (Alpha = 0.05).

Fig. 7. Percentage of attached cells on anodic oxides normalized by number of attached cells cultured on the surfaces of pretreated Ti for 1 h, $*p<0.05$.

higher voltages indicated enhanced cell attachment in either electrolyte.

As indicated in Fig. 8, the cell spreading assay demonstrated no statistical significant difference concerning the percentages of fully spread cells between the control and the different anodized surfaces at 1 hour. According to statistical analysis, at 2 h, attached cells on G-2 and G-8 displayed noticeably fewer fully spread cells than on the control, and G-8 had the lowest spreading percentage.

3.4. Morphology of cells

Fig. 9 shows fully spread cells on various surfaces at 1 and 2 h. Three kinds of fully spread cell morphologies were shown, that is, a polygonal shape; a polarized shape, i.e. elongated in the opposite directions, mostly occurring in cells on the oxides formed in electrolyte No. 1; and a round one as appeared on the control. At 1 h, most of fully spread cells on the control were round; while cells adhered on G-2, G-4 and G-8 became

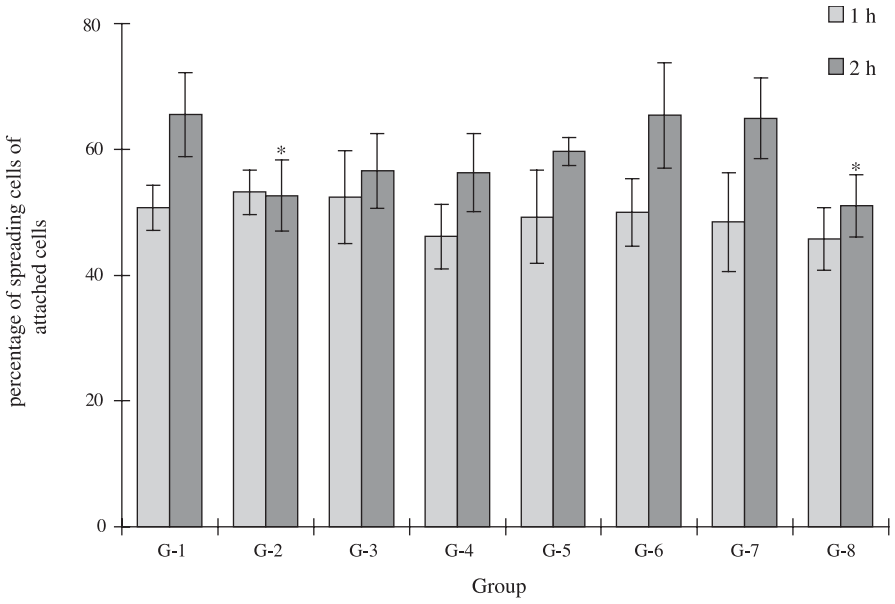

Comparisons for all pairs in the same electrolyte using Tukey-Kramer HSD (Abs(Dif)-LSD) (2 h)

	G-2	G-3	G-4		G-5	G-6	G-7	G-8
G-2	-10.055	-6.113	-6.407	G-5	-10.741	-4.979	-5.531	-2.101
G-3	-6.113	-10.055	-9.761	G-6	-4.979	-10.741	-10.189	3.661^{+}
G-4	-6.407	-9.761	-10.055	G-7	-5.531	-10.189	-10.741	3.109^{+}
				G-8	-2.101	3.661^{+}	3.109^{+}	-10.741

$^{+}$ Positive values show pairs of means that are significantly different (Alpha = 0.05).

Fig. 8. Percentage of spread cells of attached cells on the surfaces of pretreated Ti and anodized titanium, $^{*}p<0.05$.

irregular and polygonal. At 2 h, the morphology of the fully spread cells on the control was not yet changed much and only few cells showed irregular extensions though the number of fully spread cells on the control surface was significantly increased.

After 1 and 2 h, lots of focal contacts were shown on the control, while cells on anodized surfaces with high voltages such as G-4, G-7 and G-8 developed the fewest number of focal contacts. The formation and development of focal contacts are probably affected by surface morphology. More irregular pores on these groups may reduce the formation of the observed focal contacts.

As illustrated in Fig. 10, after 1 h of cell culture, the actin cytoskeleton in most of the cells on the surface of the control was not well organized, and lamellipodia supported by the circumferential actin cytoskeleton were formed. Among all the surfaces, the stained lamella were most intensely displayed along the perimeters of the cells on the control and G-5. However, on the surfaces of G-2, G-4 and G-8, cells were multipolar and their edge was invisible. At 2 h, the actin cytoskeleton was well organized for the cells on all the surfaces. Thus, the time-dependant organisation of the actin cytoskeleton is influenced by the different anodized surfaces. On the surfaces of the control and G-5 many thick stress fibres, i.e. long bundles of assembled actin filaments, crossing the whole cell were viewed, and however, on the surfaces of other groups no apparent stress fibres were observed in cells.

3.5. Proliferation and alkaline phosphatase (ALP) activity

As shown in Fig. 11, there was no statistical difference between the control and anodized surfaces for cell proliferation after 1 and 2 days except G-7. At day 4, higher cell proliferation compared to that on the control was statistically shown on almost all the anodized surfaces except for G-2 and G-5.

No statistical difference of ALP activity was found between the control and anodized surfaces after cell culture for 1 or 2 days (Fig. 12). At day 4, the ALP activity of cells on G-6 was statistically lower than on the control and other anodized surfaces. With the increase of culturing time, the ALP activity decreased. This can be attributed to the preponderance of the proliferation of cells over the production of ALP activity.

4. Discussion

The surface properties of an implant play a critical role in the biological responses it induces and its ultimate success. In the present study, anodic oxidation

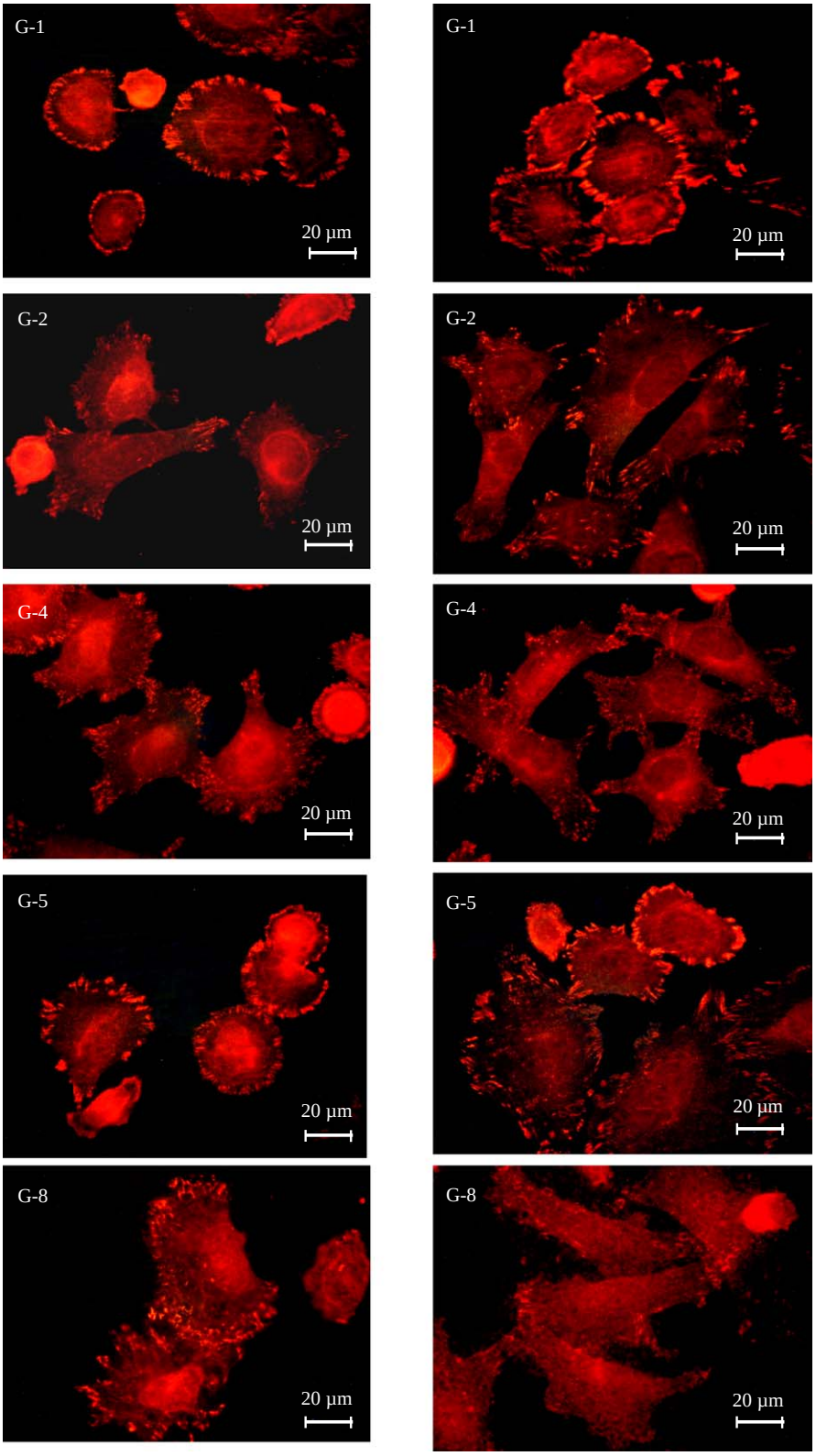

Fig. 9. Focal adhesions of cells cultured for 1 (left) and 2 h (right) on the different surfaces of titanium were stained with anti-vinculin. (G-1) pretreated Ti; (G-2) anodized at 200 V in 0.2 M H_3PO_4; (G-4) anodized at 350 V in 0.2 M H_3PO_4; (G-5) anodized at 140 V in 0.03 M Ca-GP and 0.15 M CA; (G-8) anodized at 300 V in 0.03 M Ca-GP and 0.15 M CA.

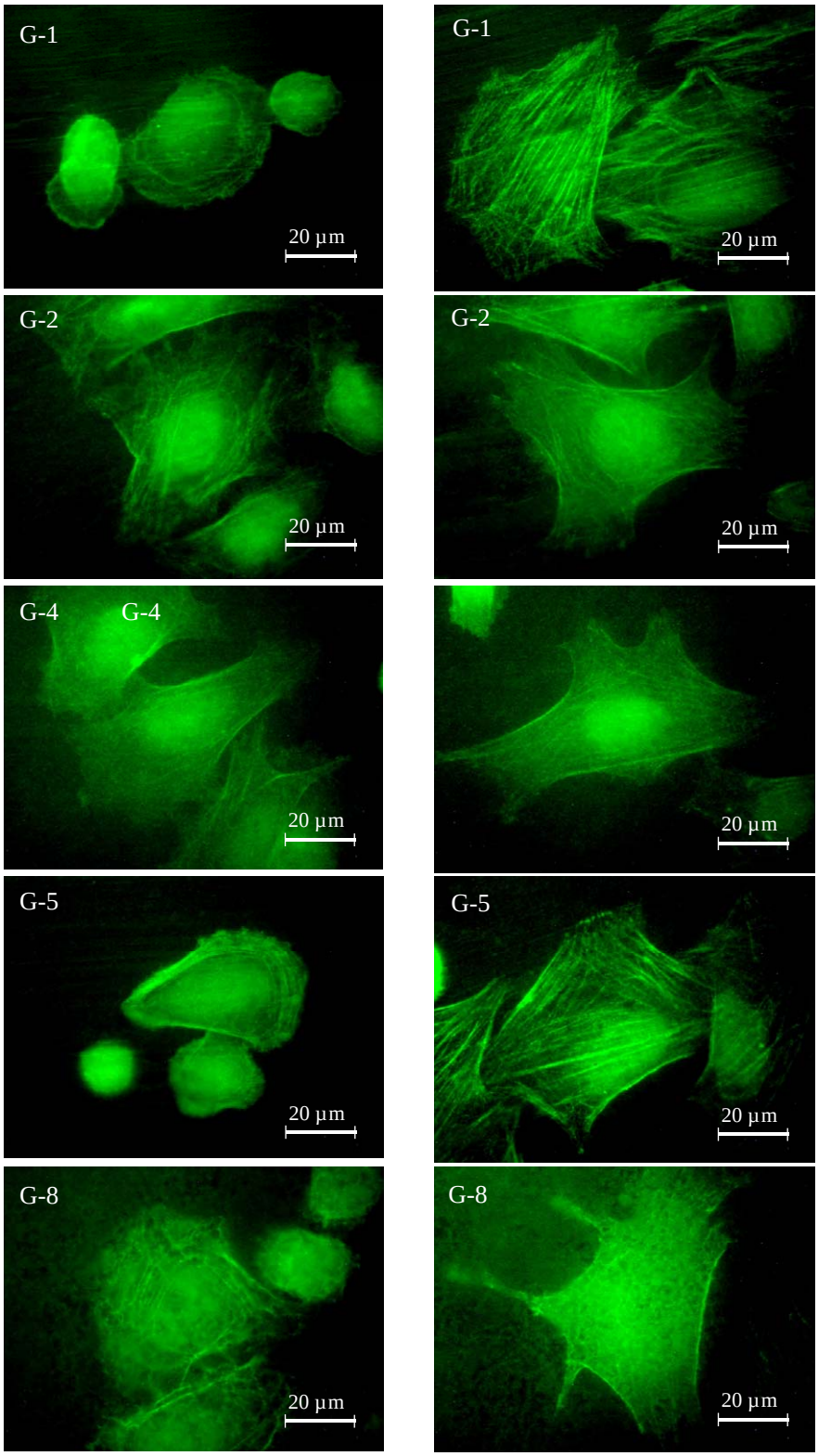

Fig. 10. Actin cytoskeleton of cells cultured for 1(left) and 2 h (right) on the different surfaces of titanium was stained with phalloidin. (G-1) pretreated Ti; (G-2) anodized at 200 V in 0.2 M H_3PO_4; (G-4) anodized at 350 V in 0.2 M H_3PO_4; (G-5) anodized at 140 V in 0.03 M Ca-GP and 0.15 M CA; (G-8) anodized at 300 V in 0.03 M Ca-GP and 0.15 M CA.

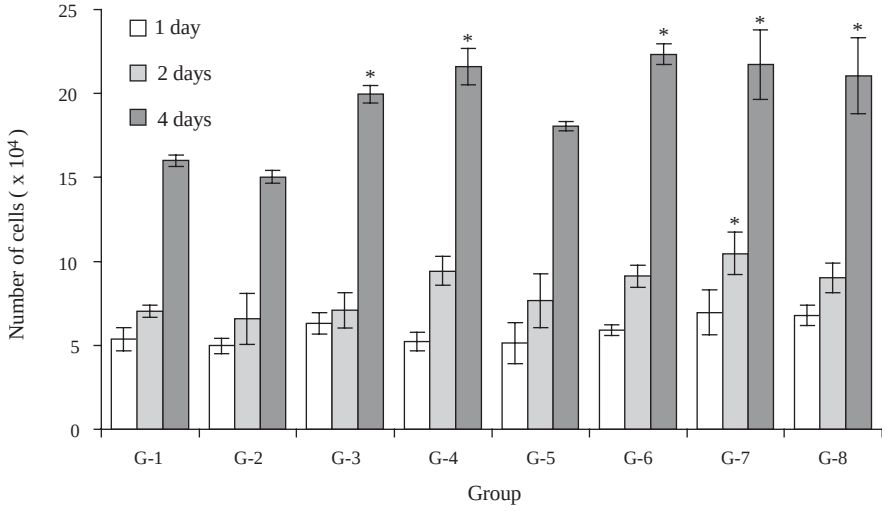

Comparisons for all pairs in the same electrolyte using Tukey-Kramer HSD (Abs(Dif)-LSD) (Day 4)

	G-2	G-3	G-4		G-5	G -6	G-7	G -8
G-2	-1.9786	2.7395^{+}	4.5914^{+}	G-5	-4.0985	0.1815^{+}	-0.4285	-1.1018
G-3	2.7395^{+}	-2.4233	-0.5938	G-6	0.1815^{+}	-4.0985	-3.4885	-2.8152
G-4	4.5914^{+}	-0.5938	-1.9786	G-7	-0.4285	-3.4885	-4.0985	-3.4252
				G-8	-1.1018	-2.8152	-3.4252	-4.0985

$^{+}$ Positive values show pairs of means that are significantly different (Alpha = 0.05).

Fig. 11. Cell proliferation on the different surfaces of titanium. Osteoblasts were seeded at 2.0×10^4 cells/cm^2 onto specimens. The culture medium was renewed every 2 days. After 1, 2 and 4 days, the medium was removed and the cells were washed with PBS, and counted with a hemocytometer. $^{*}p < 0.05$.

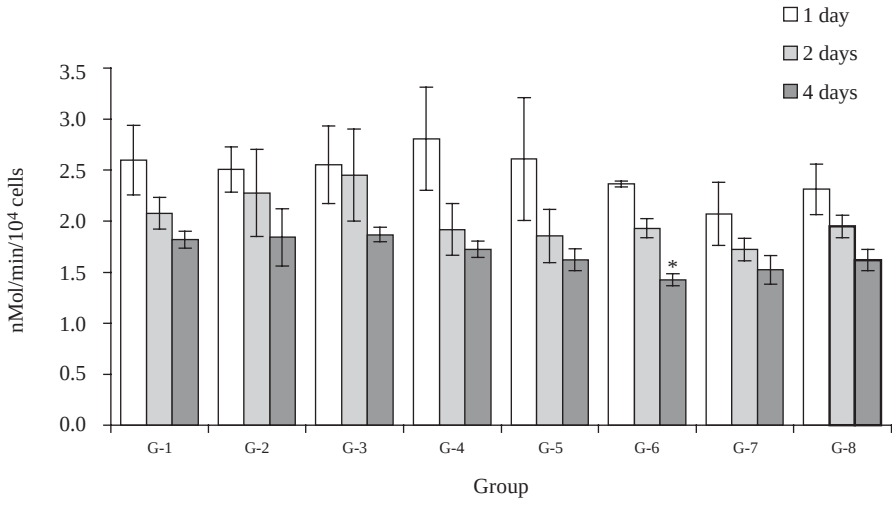

Fig. 12. Alkaline phosphatase (ALP) activity of cells on the difference surfaces of titanium for 1, 2 or 4 days. $^{*}p < 0.05$.

produces different topographies and chemical compositions of surface oxides on titanium. SEM analyses show micro-pores in the surface oxides of titanium except for the control and G-5. With an increase of anodizing voltages, the geometry of micro-pores in the anodic oxides increases in 0.2 M H_3PO_4 (up to ca. 0.5 μm) as well as in 0.03 M Ca-GP and 0.15 M CA (up to ca. 2 μm). Phosphorus and calcium are incorporated into the surface oxide on titanium by anodic oxidation in different electrolytes. The XPS analyses show that the surface oxide of titanium is TiO_2, which, as reported before, is the predominant surface oxide on top of titanium and titanium alloys, and contains small amount of suboxides TiO and Ti_2O_3 closer to the metal/oxide interface [34,35]. The content of carbon in all the surfaces is about 20 at% (30 at% at most), which is much lower than that in the surfaces of most titanium implants (about 40–80 at%) [36,37]. It is evident that the hydrocarbon cannot be present as a continuous overlayer even with carbon 43–45 at% [36]. Carbon contaminations on different oxides in our experimental groups were similar. Thus, though it cannot be ruled out

that the results of our experiments are influenced by these contaminations to some extent, the described differences between the various coatings and the control are obviously due to the different oxides rather than to surface contaminations. In the present experiments, the comparatively low surface contamination is ascribed to the acid cleaning in the pre-treatment, anodizing and deionized-water washing. Particularly, acid cleaning and anodizing efficiently remove the outer layer formed during machining by etching or dissolving due to sparking in anodizing. From O 1s, P 2p and Ca 2p spectra, it is suggested that phosphorus in the anodized surfaces formed in both electrolytes be in the form of phosphate, and besides, calcium in the anodic oxides formed in electrolyte No. 2 take the form of calcium phosphate. The existence states of calcium and phosphorus incorporated into the anodic oxides are intimately associated with their sources, i.e. constitutes of electrolytes employed. Phosphorus is in the form of phosphate ions in electrolyte No. 1. In electrolyte No. 2, calcium glycerophosphate mainly consists of calcium α-glycerophosphate and calcium β-glycerophosphate, and both have calcium ions and phosphate groups in crystal structure [38]. Variation in chemical composition of the implant surface is acknowledged to affect cell attachment and proliferation [14,39,40]. The absence of cytotoxicity documents the cytocompatibility of the surface oxides containing P or Ca and P in the present chemical states. The enhanced cell attachment and proliferation on these surfaces compared to those on the control surface further confirm their improved cytocompatibility. The observed positive effects in vitro may be due to the incorporation of phosphate ions or both calcium and phosphate ions, resulting in release of calcium and/or phosphate ions or molecules that can penetrate the cell membrane or activate membrane-bound receptors [41]. Besides, recent in vivo studies demonstrate a much higher percentage of bone contact for titanium implants with anodic oxides incorporated with both Ca and P or P, respectively, than the control [21,42], and this is explained by the formation of biochemical bonding in the bone-implant interface between bone and anodized surfaces, which have Ca and P incorporated [42].

Cell attachment, spreading and subsequent proliferation are closely related to the surface properties of the substrate, e.g. composition, roughness, wettability and morphology. Besides chemical composition, as aforementioned, it is well known that surface roughness and morphology play an important role in biological responses of biomaterial surfaces. Surface roughness is enhanced by anodic oxides within the range of 0.1–0.5 μm and differs with anodizing voltages in two different electrolytes. The roughness variation can be explained by two contradictory mechanisms, i.e. decreasing roughness by removing grooves and increasing roughness by forming irregular pores. Thus, the increase of voltage leads to two possible results, i.e. decrease or increase of roughness, depending on which of the two contradictory mechanisms is dominant, that is, disappearance of grooves and pore formation. As anodizing voltage increased, the decrease of roughness resulting from removing polishing grooves is beyond the roughness increase derived from pores, whose contribution is weak due to small pore's diameter (ca. 0.5 μm at most) for electrolyte No. 1. In contrast, the pore formation led to an increase in roughness in electrolyte 2 due to much larger pores (diameter up to ca. 2 μm at 300 V) formed in this electrolyte.

Surface wettability may affect the attachment of cells either directly, since the attachment phase as an initial process involves physicochemical linkages between cells and surfaces including ionic forces or indirectly through alterations in the adsorption of conditioning molecules, e.g. proteins. Increased wettability enhances interaction between implant surfaces and the biologic environment [43–46]. Surface wettability is affected not only by surface chemistry but also by topography parameters such as roughness and micro-texture. In the present work, all the surfaces are hydrophilic as the values of contact angles are in the range of 60–90°, which is similar to other researchers' results [3,47]. This means that all the surfaces in the present study are conducive to cell attachment since it is revealed that mammalian cells can efficiently attach to hydrophilic surfaces in comparison with hydrophobic surfaces the cells inefficiently attach to [48]. From the present experimental data, no correlation of contact angles and cell responses is demonstrated. A number of investigations have been undertaken on the influence of surface roughness on wettability parameters by static and dynamic contact angle measurements [3,49,50]. It is mainly concluded that roughness decreases the contact angle if the surface contact angle $\theta < 90°$ and increases the contact angle if $\theta > 90°$ [51]. The phenomenon that roughness decreases contact angles is also found in the present anodized surfaces except for G-5. This could be explained from the analysis of surface topography i.e. micro-texture and surface composition. Except for G-5, which indicates grooved morphology, all the other anodized surfaces are porous. For the porous surfaces, as Bico et al. [50] suggested, in the hydrophilic case, the water drop either follows the topography, which generates an efficient decreasing of the contact angle, or it spreads inside the pores, which also leads to the decrease of the contact angle.

Besides morphological parameters, surface composition should also be considered as a factor in the discussion of contact angles of the surface oxides. Ions Ca^{2+} and PO_4^{3-}, as hydrophilic components in the surface oxides, promote surface hydration resulting in a decrease of contact angles. The compositional factor

obviously has no effect in electrolyte No. 1, because the content of phosphate ions keeps almost constant in the oxides formed in this electrolyte. In electrolyte No 2, influence of the compositional effect cannot be distinguished from morphological effects since both Ca^{2+} and PO_4^{3-} contents in the oxides become higher by enhancing anodizing voltages, but this is also accompanied by an increase of roughness.

From statistical analyses, cell attachment distinctly shows different results with the change of surface roughness. In 0.2 M H_3PO_4, cell attachment on the anodized surfaces increases with a decrease in roughness. On the contrary, in 0.03 M Ca-GP and 0.15 M CA, cell attachment is increased as roughness is enhanced. However, attached cells on the surfaces anodized in either electrolyte increase with an increase in anodizing voltages, which are, in turn, associated with the thickness and topography of the surface oxide. Similar contradictory phenomena have been also observed on titanium, i.e. the increase as well as decrease of osteoblast attachment and proliferation on rougher surfaces of titanium [11,52–54]. The disagreements between cell adhesion and surface roughness, in fact, further confirm that multiple characteristics of surface oxides of titanium are involved in cell responses. The thickness of the surface oxide, among the surface characteristics, is shown to be a main factor influencing the cell response besides surface roughness [15,55]. In vivo studies show that a high degree of bone contact and bone formation are achieved with titanium implants which are modified with respect to oxide thickness and surface topography [56], and a significantly stronger bone response to anodic titanium oxides with 0.6–1.0 μm thickness than those with 0.2 μm or less thickness [7]. Anodic oxide film thickness is linearly dependent on the applied voltage for titanium [57]. As anodizing voltage increases, the thickness and crystallinity of the anodic oxides increase [8], and the thicker oxide with higher stability leads to favourable cell adhesion [4,5]. In the present study, additionally, surface micro-pores of anodic oxides formed at higher anodizing voltages probably provide some benefits for cell attachment though the detailed mechanism has yet to be investigated. Consequently, cell attachment on the anodic oxides formed in 0.2 M H_3PO_4 is enhanced even with a little decrease in roughness. In 0.03 M Ca-GP and 0.15 M CA, in contrast, as anodizing voltage increases, the roughness, number and size of micro-pores and thickness as well as the crystallinity of anodic oxides gradually increase [10]. Hence, cell attachment is enhanced accompanying with the increase of roughness, micro-pore number and size, and thickness.

After the spherical cells attach on the surfaces, the following event for cell-substrate interaction is cell spreading. The substratum surface topography alters cell shape and modulates fibronectin at the transcriptional and post-transcriptional levels, as well as the amount of fibronectin assembly into the extracellular matrix [58]. It is reported that the surface texture of the Ti substrate can also affect the expression of fibronectin and vitronectin integrin receptors [59], modify their clustering or aggregation, and therefore determine variations in shape and spreading of cells [53]. During cell spreading, the shape of cells is changed and the cellular skeleton is reorganized. In our experiments, the shape of cells on the control surface and anodized surfaces is distinctly different, though the percentage of fully spread cells to total attached cells shows no statistical difference. This can be explained by the reason that cell spreading is affected by surface morphology or micro-topography. Most spread cells on the control surface after 1 h are round, which is the same appearance as described on smooth surfaces [60], while the cells on the anodized titanium surface appeared more irregular and polygonal, covering a larger mean surface area, especially on G-4, G-7 and G-8. Since spreading is an essential step in cell adhesion prior to exponential growth phase [61], cell spreading can have a profound effect on cell adhesion and growth. In fact we also see in our experiments that cell proliferation is enhanced by oxide surfaces leading to a more rapid and distinct polygonal spreading of the cells. It is reported that cells appear to be under precise control by topographic guidance cues of various dimensions during morphogenesis [62]. However, little is known about the mechanisms whereby surface topography exerts its effects on cell shape and further growth [58].

In the present study, focal contacts on the control are more intensive than on anodized groups. Focal contacts act as a special structure of cell adhesion on the substrates, but in general, cells that form strong focal adhesions are less migratory. The shallow appearance of focal contacts on the more intensively anodized surfaces indicates that cell migration may be easier than on the control surface. Many more lamellipodia involved in cell migration are observed in cells on the more intensively anodized titanium than on the control. These phenomena indicate that the ability of cell migration on anodic oxides may be higher than that on the control and increases as anodizing voltage increases. In the present study, more stress fibers but fewer lamellipodia were formed on the control or weakly anodized surfaces. As a highly organized cytoskeleton with stress fibers is often associated with strong cell adhesion [63], the reorganization of the actin cytoskeleton, together with the results of the amount and distribution of focal contacts, further confirm the assumption that the cells on anodic oxides may have higher motility in comparison with those on the control.

The present results show, on the whole, that cell proliferation is enhanced by anodic oxidation. In 0.2 M

H_3PO_4, rougher surfaces exhibit lower cell proliferation and this is consistent with the results from Martin et al. [15]. On the other hand, some researchers presented the different relationship, i.e. osteoblast proliferation could be enhanced on rougher surfaces [51,64]. In 0.03 M Ca-GP and 0.15 M CA, cell proliferation has no statistical difference except between G-5 and G-6. Therefore, cell proliferation is not only affected by roughness but also by surface micro-structure, composition and thickness of anodic oxides.

From the ALP activity in the present work, no apparent correlation is shown between surface characteristics and osteoblast differentiation. The contradictory relationship reported for cell proliferation or ALP activity and roughness can be ascribed to the sensitivity of osteoblasts to the surface features such as surface micro-topography [11,65,66].

5. Conclusions

In the present study, surface oxides of titanium were varied in topography and chemical composition by anodic oxidation in 0.2 M H_3PO_4, and in 0.03 M Ca-GP and 0.15 M CA. P (ca.10 at%) or Ca (1–6 at%) and P (3–6 at%) were incorporated into the surface oxides and by anodic oxidation, surface roughness became lower in 0.2 M H_3PO_4 but enhanced in 0.03 M Ca-GP and 0.15 M CA. Phosphorus and calcium existed in the form of phosphate and calcium phosphate, respectively, in the anodic oxides. Anodized surfaces showed micro-pores with diameters up to 0.5 μm in 0.2 M H_3PO_4 and to 2 μm in 0.03 M Ca-GP and 0.15 M CA. Contact angles of anodic oxides ranges from 60 to 90°. Cell culture experiments demonstrated lack of cytotoxicity. Cells on anodic oxides showed irregular, polygonal growth and developed a number of lamellipodia. Cells on the control titanium surface or the anodic oxides formed at low voltages, on the other hand, showed many thick stress fibres and intense focal contacts. Cell attachment as well as cell proliferation was enhanced by the anodic oxides. Cell attachment increased as anodizing voltage or thickness of oxides, number and size of micro-pores, and roughness increased. ALP activity of the cells was not influenced by the surface characteristics of the anodic oxides under our experimental conditions.

Acknowledgements

The work was financially supported by the Fortuene Foundation (No. 989-0-0, Medical Clinic, University of Tuebingen). The authors gratefully acknowledge the assistance of Ms. Christine Schille in measurement of roughness, Mrs. Evi Kimmerle in cell culture as well as Prof. Wolfgang Lindemann in SEM.

References

[1] Williams DF. Titanium and titanium alloys. In: Williams DF, editor. Biocompatibility of clinical implant materials, vol. I. Boca Raton, Florida: CRC Press, Inc.; 1981. p. 9–44.
[2] Lampin M, Warocquier-Clerout R, Legris C, Degrange M, Sigot-Luizard MF. Correlation between substratum roughness and wettability, cell adhesion, and cell migration. J Biomed Mater Res 1997;36:99–108.
[3] Lim YJ, Oshida Y, Andres CJ, Barco MT. Surface characterization of variously treated titanium materials. Int J Oral Maxillofac Implants 2001;16:333–42.
[4] Keller JC, Stanford CM,Wightman, Draughn JP, Zaharias RA. Characterization of titanium implant surfaces. III. J Biomed Mater Res 1994;28:939–46.
[5] Kieswetter K, Schwartz Z, Dean DD, Boyan BD. The role of implant surface characteristic in the healing of bone. Crit Rev Oral Biol Med 1996;7:329–45.
[6] Pouilleau J, Devilliers D, Garrido F, Durand-Vidal S, Mahe E. Structure and composition of passive titanium oxide films. Mater Sci Eng 1997;B47:235–43.
[7] Sul YT, Johansson CB, Jeong Y, Wennerberg A, Albrektsson T. Resonance frequency and removal torque analysis of implants with turned and anodised surface oxides. Clin Oral Impl Res 2002;13:252–9.
[8] Zhu X, Kim K, Ong JL, Jeong Y. Surface analysis of anodic oxide films containing phosphorus on titanium. Int J Oral Maxillofac Implants 2002;17:331–6.
[9] Zhu X, Ong JL, Kim S, Kim K. Surface characteristics and structure of anodic oxide films containing Ca and P on a titanium implant material. J Biomed Mater Res 2002;60:333–8.
[10] Zhu X, Kim K, Jeong Y. Anodic oxide films containing Ca and P of titanium biomaterial. Biomaterials 2001;22:2199–206.
[11] Lincks J, Boyan BD, Blanchard CR, Lohmann CH, Liu Y, Cochran DL, Dean DD, Schwartz Z. Response of MG63 osteoblast-like cells to titanium and titanium alloy is dependent on surface roughness and composition. Biomaterials 1998;19:2219–32.
[12] Letic-Gavrilovic A, Scandurra R, Abe K. Genetic potential of interfacial guided osteogenesis in implant devices. Dent. Mater J 2000;19:99–132.
[13] Eriksson C, Lausmaa J, Nygren H. Interactions between human whole blood and modified TiO_2-surfaces: influence of surface topography and oxide thickness on leukocyte adhesion and activation. Biomaterials 2001;22:1987–96.
[14] Brunette DM. The effects of implant surface topography on the behavior of cells. Int J Oral Maxillofac Implants 1988;3:231–46.
[15] Martin JY, Schwartz Z, Hummert TW, Schraub DM, Simpson J, Lankford Jr J, Dean DD, Cochran DL, Boyan BD. Effect of titanium surface roughness on proliferation, differentiation, and protein synthesis of human osteoblast-like cells (MG63). J Biomed Mater Res 1995;29:389–401.
[16] MacDonald DE, Deo N, Markovic B, Stranick M, Somasundaran P. Adsorption and dissolution behavior of human plasma fibronectin on thermally and chemically modified titanium dioxide particles. Biomaterials 2002;23:1269.
[17] Maxian SH, Zawadsky JP, Dunn MG. Effect of Ca/P coating resorption and surgical fit on the bone/implant interface. J Biomed Mater Res 1994;28:1311–9.
[18] Cheung HS, McCarty DJ. Mitogenesis induced by calcium-containing crystals. Role of intracellular dissolution. Exp Cell Res 1985;157:63–70.
[19] Basle MF, Chappard D, Grizon F, Filmon R, Delecrin J, Daculsi G, Rebel A. Osteoclastic resorption of Ca-P biomaterials implanted in rabbit bone. Calcif Tissue Int 1993;53:348–56.

[20] Zhu X, Chen J, Scheideler L, Schille C, Geis-Gerstorfer J. In vitro osteoblast responses to anodic oxides containing Ca and P on titanium. J Dent Res 2003;82:B-308, 2379.
[21] Son W, Zhu X, Shin H, Ong JL, Kim K. In vivo histological response to anodized and anodized/hydrothermally treated titanium implants. J Biomed Mater Res Part B: Appl Biomater 2003;66B:520–5.
[22] Baier RE, Meyer AE, Natiella JR, Carter JM. Surface properties determining bioadhesive outcome: methods and results. J Biomed Mater Res 1984;18:337–55.
[23] Albrektsson T, Branemark P-I, Hansson H-A, Lindstroem J. Osseointegrated titanium implants. Act Orthopaedica Scandinavica 1981;52:155–70.
[24] Vezeau P, Keller J, Wightman J. Reuse of healing abutments: an in vitro model of plasma cleaning and common sterilization techniques. Implant dentistry 200;9:236–46.
[25] Rajaraman R, Rounds DE, Yen SP, Rembaum A. A scanning electron mircroscope study of cell adhesion and spreading in vitro. Exp Cell Res 1974;88:327–39.
[26] Wennerberg A, Albrektsson T, Johansson C, Andersson B. Experimental study of turned and grit-blasted screw-shaped implants with special emphasis on effects of blasting material and surface topography. Biomaterials 1996;17:15–22.
[27] Dupraz A, Nguyen TP, Richard M, Daculsi G, Passuti N. Influence of a cellulosic ether carrier on the structure of biphasic calcium phosphate ceramic particles in an injectable composite material. Biomaterials 1999;20:663–73.
[28] Carley AF, Roberts JC, Roberts MW. Dissociative chemisorption and localized oxidation states at titanium surfaces. Surf Sci 1990;225:L39–41.
[29] Beamson G, Briggs D. High-resoultion XPS of organic polymers; the science ESCA 300 database. Wiley: Chichester, UK; 1992.
[30] Sham TK, Lazarus MS. X-ray photoelectron spectroscopy (XPS) studies of clean and hydrated TiO_2 (rutile) surfaces. Chem Phys lett 1979;68:426–32.
[31] Lu G, Bernasek SL, Schwartz J. Oxidation of a polycrystalline titanium surface by oxygen and water. Surf Sci 2000;458:80–90.
[32] Viornery C, Chevolot Y, Leonard D, Aronsson BO, Pechy P, Mathieu HJ, Descouts P, Graetzel M. Surface modification of titanium with phosphonic acid to improve bone bonding: characterization by XPS and ToF-SIMS. Langmuir 2002; 18:2582–9.
[33] Charles C C, Goodman DW. Calcium phosphate phase identification using XPS and time-of-flight cluster SIMS. Anal Chem 199;71:149–53.
[34] Feng B, Weng J, Yang BC, Qu SX, Zhang XD. Characterization of surface oxide films on titanium and adhesion of osteoblast. Biomaterials 2003;24:4663–70.
[35] Ask M, Lausmaa, Kasemo B. Preparation and surface spectroscopic characterization of oxide films on Ti6Al4 V. Appl Surf Sci 1988–89;35:283–301.
[36] Ameen AP, Short RD, Johns R, Schwach G. The surface analysis of implant materials. Clin Oral Impl Res 1993;4:144–50.
[37] Morra M, Cassinelli C, Bruzzone G, Carpi A, Santi GD, Giardino R, Fini M. Surface chemistry effects of topographic modification of titanium dental implant surfaces: 1. surface analysis. Int J Oral Maxillofacial Implants 2003;18:40–5.
[38] Inoue M, In Y, Ishida T. Calcium bionding to phospholid: structural study of calcium glycerophosphyte. J Lipid Res 1992;33:985–94.
[39] Sinha RK, Morris F, Shah SA, Tuan RS. Surface composition of orthopaedic implant metals regulates cell attachment, spreading, and cytoskeletal organization of primary human osteoblasts in vitro. Clin Orthop 1994;305:258–72.
[40] Morra M, Cassinelli C, Bruzzone G, Carpi A, Di Santi G, Giardino R, Fini M. Surface chemistry effects of topographic modification of titanium dental implant surfaces: 1. surface analysis. Int J Oral Maxillofac Implants 2003;18:40–5.
[41] Kasemo B, Gold J. Implant surfaces and interface processes. Adv Dent Res 1999;13:8–20.
[42] Sul YT. The significance of the surface properties of oxidized titanium to the bone response: special emphasis on potential biochemical bonding of oxidized titanium implant. Biomaterials 2003;24:3893–907.
[43] Dexter SC. Influence of substratum critical surface tension on bacteria adhesion-in situ studies. J Colloid Interface Sci 1979; 70:346–54.
[44] Baier RE, Shafrin EG, Zisman. Adhesion: mechanisms that assist or impede it. Science 1968;162:1360–8.
[45] Schrader ME. On adhesion of biological substances to low energy solid surface. J Colloid Interface Sci 1982;88:296–7.
[46] Baier RE, Meyer AE, Natiella JR, Natiella RR, Carter JM. Surface properties determine bioadhesive outcomes: methods and results. J Biomed Mater Res 1984;18:337–55.
[47] Takebe J, Itoh S, Okada J, Ishibashi K. Anodic oxidation and hydrothermal treatment of titanium results in a surface that causes increased attachment and altered cytoskeletal morphology of rat bone marrow stromal cells in vitro. J Biomed Mater Res 2000;51:398–407.
[48] Vogler EA. Structure and reactivity of water at biomaterial surfaces. Adv Colloid Interface Sci 1998;74:69–117.
[49] Bico J, Tordeux C, Quere D. Rough wetting. Europhys Lett 2001;55:214–20.
[50] Bico J, Thiele U, Quere D. Wetting of textured surfaces. Colloids and Surfaces A: Physciochem Eng Aspects 2002;206: 41–6.
[51] Borgs C, De Coninck J, Kotecky R, Zinque M. Does the roughness of the substrate enhance wetting? Phys Rev Lett 1995;74:2292–4.
[52] Bowers KT, Keller JC, Randolph BA, Wick DG, Michaels CM. Optimization of surface micromorphology for enhanced osteoblast responses in vitro. Int J Oral Maxillofac Implants 1992;7: 302–10.
[53] Degasne I,Basle, Demais ME, Hure V, Lesourd G, Grolleau M, Mercier B, Chappard L. Effects of roughness, fibronectin and vitronectin on attachment, spreading, and proliferation of human osteoblast-like cells (Saos-2) on titanium surface. Calcif Tissue Int 1999;64:499–507.
[54] Mustafa K, Wennerberg A, Wroblewski J, Hultenby K, Lopez BS, Arvidson K. Determining optimal surface roughness of TiO_2 blasted titanium implant material for attachment, proliferation and differentiation of cells derived from human mandibular alveolar bone. Clin Oral Impl Res 2001;12:515–25.
[55] Anselme K, Linez P, Bigerelle M, Le Maguer D, Le Maguer A, Hardouin P, Hildebrand HF, Iost A, Leroy JM. The relative influence of the topography and chemistry of TiAl6V4 surfaces on osteoblastic cell behaviour. Biomaterials 2000; 21:1567–77.
[56] Larsson C, Thomsen P, Aronsson BO, Rodahl M, Lausmaa J, Kasemo B, Ericson LE. Bone response to surface-modified titanium implants: studies on the early tissue response to machined and electropolished implants with different oxide thicknesses. Biomaterials 1996;17:605–16.
[57] Lausmaa J, Kasemo B, Mattsson H, Odelius H. Multitechnique surface characterization of oxide films on electroplished and anodically oxidized titanium. Appl Surf Sci 1990; 45:189–200.
[58] Chou L, Firth J, Uitto V, Brunette D. Substratum surface topography alters cell shape and regulates fibronectin mRNA level, mRNA stability,secretion and assembly in human fibroblasts. J Cell Sci 1995;108:1563–73.

[59] Hormia M, Kononen M. Immunolocalization of fibronectin and vitronection receptors in human gingival fibroblasts spreading on titanium surfaces. J Periodontal Res 1994;29:146–52.
[60] Brunette DM. Principles of cell behavior on titanium surfaces and their application to implanted devices. In: Brunette DM, Tengvall P, Textor M, Thomsen P, editors. Titanium in medicine. Berlin: Springer; 2001. p. 485–512.
[61] Vogler EA, Bussian RW. Short-term cell-attachment rates. A surface-sensitive test of cell-substrate compatibility. J Biomed Mater Res 1987;21:1197–211.
[62] Curtis ASG, Clark P. The effects of topographic and mechanical properties of materials on cell behavior. Crit Rev Biocomp 1990;5:343–62.
[63] Badley RA, Woods A, Carruthers L, Rees DA. Cytoskeletal changes in fibroblast adhesion and detachment. J Cell Sci 1980;43:379–90.
[64] Hatano K, Inoue H, Kojo T, Matsunago T, Tsujisawa T, Uchiyama C, Uchida Y. Effect of surface roughness on proliferation and alkaline phosphatase expression of rat calvarial cells cultured on polystyrene. Bone 1999;25:439–45.
[65] Groessner-Schreiber B, Tuan RS. Enhanced extracellular matrix production and mineralization by osteoblasts cultured on titanium surfaces in vitro. J Cell Sci 1992;101: 209–17.
[66] Davies JE, Lowenberg B, Shiga A. The bone-titanium interface in vitro. J Biomed Mater Res 1990;24:1289–306.